

# Cyclotron effects on wave dispersion in pulsar plasmas

M. P. KENNETT,<sup>\*</sup> D. B. MELROSE and Q. LUO

Research Centre for Theoretical Astrophysics, School of Physics, University of Sydney,  
NSW 2006, Australia

(Received 28 February 2000)

**Abstract.** Dispersion in an intrinsically relativistic, one-dimensional, electron–positron pair plasma (a pulsar plasma) is treated exactly, generalizing earlier results that applied in the low-frequency limit and that neglected the cyclotron resonance. The general theory involves two additional relativistic plasma dispersion functions, evaluated at the normal and anomalous Doppler resonances. These two functions are associated with the non-gyrotropic and gyrotropic parts of the response respectively. The functions are evaluated for bell-type and Jüttner distributions. Wave dispersion is discussed for a non-gyrotropic pulsar plasma with a highly relativistic Alfvén speed. Emphasis is placed on crossings of the light line, defined in terms of the parallel phase velocity. Subluminal waves exist only for sufficiently small angles of propagation, and are confined to frequencies below about the mean gyrofrequency of the relativistic particles.

---

## Dedication

This paper is dedicated to John Dougherty on the occasion of his 65th birthday.

## 1. Introduction

Low-frequency waves in an extremely strongly magnetized, highly intrinsically relativistic, one-dimensional, electron–positron pair plasma (a pulsar plasma) are of interest in theories for the radio emission from pulsars (see e.g. Tsytovich and Kaplan 1972; Melrose and Stoneham 1997; Allen and Melrose 1982; Gedalin and Machabeli 1983; Volotkin et al. 1985; Arons and Barnard 1986; Lyutikov 1998). In earlier papers (Gedalin et al. 1998, hereinafter GMG; Melrose et al. 1999, hereinafter MGKF) the properties of waves were described for a pulsar plasma in the low-frequency limit, corresponding to frequencies well below the cyclotron resonance. In the present paper, we extend the theory to include the cyclotron resonance. The one-dimensionality of the plasma is due to all the particles being in the ground state of their spiralling motion ('lowest Landau orbital'  $l = 0$ ) owing to their perpendicular energy being radiated away through gyromagnetic emission; cyclotron effects involve transitions from the ground state,  $l = 0$ , to  $l = 1$ , where  $l$  is a simple harmonic oscillator quantum number, with these transitions being virtual for the reactive effects and real for dissipative effects. Three consequences

<sup>\*</sup> Present address: Princeton University.

of the cyclotron resonance are of interest. First, reactive cyclotron effects modify the properties of the wave modes, and in principle can lead to intrinsically new modes that have no counterpart at low frequencies. Secondly, cyclotron absorption can modify the escaping radiation (Mikhailovskii et al. 1982), perhaps imposing a circular polarization on it due to preferential absorption by either electrons or positrons. Thirdly, an anomalous Doppler instability is possible in principle (Lominadze et al. 1983; Machabeli and Usov 1989; Kazbegi et al. 1991), and might lead to observable consequences.

Our main purpose in this paper is to extend the formal theory of dispersion in a pulsar plasma to allow all these effects to be treated. In discussing the specific consequences, we concentrate on the effect of the cyclotron resonance on dispersion, emphasizing the case of very high Alfvén speeds,  $v_A \gg 1$  (in units with  $c = 1$ ). Compared with a non-relativistic pair plasma, where the cyclotron resonance leads to a resonance ( $|\mathbf{k}| \rightarrow \infty$ ) in the wave dispersion, the spread in cyclotron frequencies in an intrinsically highly relativistic plasma smooths out the cyclotron effects on the dispersion. At frequencies well above the cyclotron resonance, one expects  $\omega > |\mathbf{k}|$  for all waves, and hence that the dispersion curves for waves modes that have  $\omega < |\mathbf{k}|$  at low frequency should cross the light line near the cyclotron resonance. It is more relevant to consider the parallel phase speeds,  $z = \omega/k_{\parallel}$ , in defining whether waves are subluminal,  $z < 1$ , or superluminal,  $z > 1$ . This is because (for a one-dimensional plasma) only subluminal waves can satisfy the Landau and anomalous Doppler resonance conditions, and hence only these waves can be generated by the two available types of instability in a one-dimensional plasma. The only specific application of the general theory that we consider in this paper concerns the conditions under which waves exist with  $z < 1$ .

In Sec. 2, we show that the normal and anomalous cyclotron resonances define two parallel phase velocities, which play an important role in the subsequent theory. In Sec. 3 the relativistic plasma dispersion functions (RPDFs) that appear in the theory are defined, and these are evaluated for explicit choices of distribution function in Sec. 4. The components of the response tensor are written down in Sec. 5; quantum mechanical effects on the waves are not considered, although the particles are treated quantum mechanically in the sense that they are all in the lowest quantum state of the gyrating motion. In Sec. 6, the effect of the cyclotron resonance on the wave properties are discussed in the non-gyrotropic case, with emphasis on the conditions under which waves with  $z < 1$  exist.

## 2. The cyclotron resonance

The cyclotron resonance condition corresponds to

$$\omega - \frac{s\Omega_e}{\gamma} - k_{\parallel}v = 0, \quad (2.1)$$

where  $k_{\parallel}$  is the wavenumber along the direction of the magnetic field,  $\Omega_e = eB/m$  is the non-relativistic cyclotron frequency,  $v = v_{\parallel}$  with  $v_{\perp} = 0$  is the one-dimensional particle velocity and  $\gamma = (1 - v^2)^{1/2}$  is the Lorentz factor of the particle. Only  $s = 0$ ,  $s = 1$  and  $s = -1$  are allowed for a one-dimensional distribution of particles, and these correspond to the Landau, normal cyclotron and anomalous cyclotron resonances, respectively. In Fig. 1 we illustrate the ranges in  $(z, y)$  space, with  $z = \omega/k_{\parallel}$  and  $y = \Omega_e/k_{\parallel}$ , where these resonances are allowed: the resonance  $s = 0$

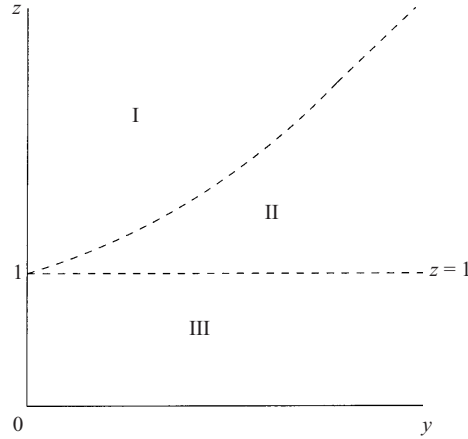


**Figure 1.** Regions of interest in  $(z,y)$  space: region I is  $z > (1 + y^2)^{1/2}$ ; region II is  $1 < z < (1 + y^2)^{1/2}$ ; region III is  $z < 1$ . Resonance at  $s = 1$  is allowed in regions II and III, and resonances at  $s = 0, s = -1$  are allowed only in region III.

and  $s = -1$  are allowed only in region III ( $z < 1$ ), the resonance at  $s = 1$  is allowed only for  $z < (1+y^2)^{1/2}$ , which is regions II and III. There is no dissipation in region I. In semiclassical language, resonance at  $s = 1$  involves absorption of a quantum of radiation with a particle jumping from its lowest Landau orbital to the first excited state, and  $s = -1$  corresponds to induced emission of a quantum of radiation with a particle jumping from its lowest Landau orbital to the first excited state. These two processes need to be distinguished when discussing the dissipative part of the plasma response, but they are treated together when discussing the reactive part of the response, which determines the wave properties of interest here.

For  $s = \pm 1$ , the resonance condition (2.1) may be written in the form

$$(\omega - k_{\parallel}v)^2 - \frac{\Omega_e^2}{\gamma^2} = k_{\parallel}^2(1 + y^2)(v - z_+)(v - z_-), \tag{2.2}$$

where the two solutions  $v = z_{\pm}$  have

$$z_{\pm} = \frac{z \pm y(1 + y^2 - z^2)^{1/2}}{1 + y^2} = \frac{\omega k_{\parallel} \pm \Omega_e(\Omega_e^2 + k_{\parallel}^2 - \omega^2)^{1/2}}{\Omega_e^2 + k_{\parallel}^2}. \tag{2.3}$$

The cyclotron resonance occurs only if these solutions are in the physical range  $v^2 < 1$ , that is, for  $-1 < z_{\pm} < 1$ . The variation of  $z_{\pm}$  with  $z$  for fixed  $y$  is illustrated in Fig. 2. In view of  $z_-(-z) = -z_+(z)$ , we need discuss only the variation of  $z_+$  with  $z$  in detail. The solution  $z_+$  increases as a function of  $z < 1$ , reaching a maximum  $z_+ = 1$  for  $z = 1$  and then decreasing for  $z > 1$  to  $z_+ = 1/(1+y^2)^{1/2}$  for  $z = (1+y^2)^{1/2}$ . For larger values of  $z$ , the solution is complex, implying that there is no cyclotron resonance in the physical range. The behaviour of  $z_+$  and  $z_-$  in various limits is summarized in Table 1.

The anomalous Doppler effect ( $s = -1$ ) is possible only for  $z < 1$ , in which case  $z = z_+$  corresponds to the anomalous Doppler effect and  $z = z_-$  corresponds to the normal Doppler effect. For  $1 \leq z \leq (1 + y^2)^{1/2}$ , both solutions,  $z = z_{\pm}$ , correspond to the normal Doppler effect.

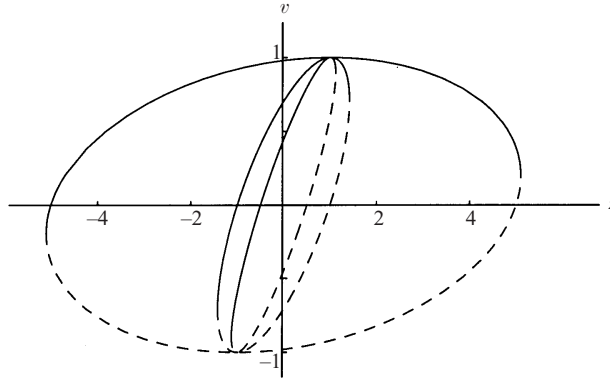


**Figure 2.** The solutions of the resonance condition (2.1) for  $v = z_+$  (solid curves) and  $v = z_-$  (dashed curves) are plotted for  $y = 0.5$  (inner ellipse),  $y = 1$  (intermediate ellipse) and  $y = 5$  (outer ellipse) as functions of  $z$ . The ellipse has its major axis along the line  $v = z$  with axial ratio  $y/(2 + y^2)^{1/2}$ .

**Table 1.** Behaviour of  $z_{\pm}$  in various limits.

Limit	Behaviour of $z_{\pm}$
$z \rightarrow 0, \quad y \rightarrow 0$	$z_{\pm} \rightarrow z \pm y$
$z \rightarrow 0, \quad z \ll y$	$z_{\pm} \rightarrow \pm \frac{y^2}{1 + y^2}$
$z \rightarrow y$	$z_+ \rightarrow \frac{2y}{1 + y^2}, \quad z_- \rightarrow 0$
$z \rightarrow 1$	$z_+ \rightarrow 1, \quad z_- \rightarrow \frac{1 - y^2}{1 + y^2}$
$y \rightarrow \infty, \quad z \ll y$	$z_{\pm} \rightarrow \pm 1$
$z \gg y, \quad z < 1$	$z_{\pm} \rightarrow \frac{z}{1 + y^2}$
$z \gg y, \quad z > 1$	$z_{\pm} \rightarrow \frac{1}{1 + y^2} [z \pm iy(z^2 - 1)^{1/2}]$
$z \rightarrow \infty, \quad z \gg y$	$z_{\pm} \rightarrow \frac{z}{1 + y^2} (1 \pm iy)$

### 3. Relativistic plasma dispersion functions

It is convenient to define averages over the (one-dimensional) particle distribution function  $f(u)$ , with  $u = p/m = \gamma v$ , by writing

$$\langle K \rangle = \int_{-\infty}^{\infty} du K f(u), \quad \int_{-\infty}^{\infty} du f(u) = 1. \tag{3.1}$$

As already remarked, the particles are treated quantum mechanically in the sense that they are all in their lowest Landau orbital; apart from the normalization, which is specified by (3.1),  $f(u)$  is equivalent to the occupation number  $N_l(p_{\parallel})$  of the lowest Landau state,  $l = 0$ , with the parallel momentum  $p_{\parallel}$  rewritten as  $p = mu$ . The plasma frequency  $\omega_p$ , the Alfvén speed  $v_A$  and a mean square speed

$\tilde{v}^2$  are defined as in GMG and MGKF:

$$\omega_p = \left( \frac{e^2 n}{\varepsilon_0 m} \right)^{1/2}, \quad v_A = \langle \gamma \rangle^{-1/2} \frac{\Omega_e}{\omega_p}, \quad \langle \gamma v^2 \rangle = \langle \gamma \rangle \tilde{v}^2, \quad (3.2)$$

where  $n$  is the sum of the number densities of electrons and positrons. The RPDFs that appear when the cyclotron resonance is taken into account are

$$W(z) = \left\langle \frac{1}{\gamma^3 (z - v)^2} \right\rangle, \quad (3.3a)$$

$$R(z) = \left\langle \frac{1}{\gamma (v - z)} \right\rangle, \quad (3.3b)$$

$$S(z) = \left\langle \frac{1}{\gamma^2 (v - z)} \right\rangle. \quad (3.3c)$$

When  $z_{\pm} = z_{\pm}^*$  is complex,  $R(z_{\pm})$  and  $S(z_{\pm})$  are given by formally extending the definitions (3.3) into the complex plane. Complex  $z_{\pm}$  appear for  $z^2 > 1 + y^2$ , when one has

$$z_{\pm} = z_0 \pm iw, \quad z_0 = \frac{z}{1 + y^2}, \quad w = \frac{y(z^2 - 1 - y^2)^{1/2}}{1 + y^2}, \quad (3.4)$$

and it is then convenient to define real functions by writing

$$R(z_{\pm}) = r_1(z_0, w) \pm iw r_2(z_0, w), \quad (3.5a)$$

$$S(z_{\pm}) = s_1(z_0, w) \pm iw s_2(z_0, w), \quad (3.5b)$$

$$r_1(z_0, w) = \left\langle \frac{v - z_0}{\gamma [(v - z_0)^2 + w^2]} \right\rangle, \quad (3.6a)$$

$$r_2(z_0, w) = \left\langle \frac{1}{\gamma [(v - z_0)^2 + w^2]} \right\rangle, \quad (3.6b)$$

$$s_1(z_0, w) = \left\langle \frac{v - z_0}{\gamma^2 [(v - z_0)^2 + w^2]} \right\rangle, \quad (3.7a)$$

$$s_2(z_0, w) = \left\langle \frac{1}{\gamma^2 [(v - z_0)^2 + w^2]} \right\rangle. \quad (3.7b)$$

In the following,  $R(z_{\pm})$  and  $S(z_{\pm})$  are to be interpreted according to (3.5)–(3.7) for  $z^2 > 1 + y^2$ .

#### 4. Components of the dielectric tensor

The response tensor is derived in the Appendix. The resulting explicit expression for the components of the dielectric tensor in a conventional 3-tensor notation, with the 3-axis along the magnetic field and  $\mathbf{k} = (k_{\perp}, 0, k_{\parallel})$  in the 1–3 plane, is

$$K_{11}(k) = K_{22}(k) = 1 - \frac{\omega_p^2}{\omega^2} \frac{1}{1 + y^2} \left[ \left\langle \frac{1}{\gamma} \right\rangle + \frac{(z - z_+)^2 R(z_+) - (z - z_-)^2 R(z_-)}{z_+ - z_-} \right], \quad (4.1a)$$

$$K_{33}(k) = 1 - \frac{\omega_p^2}{\omega^2} \left\{ z^2 W(z) + \frac{\tan^2 \theta}{1 + y^2} \left[ \left\langle \frac{1}{\gamma} \right\rangle + \frac{z_+^2 R(z_+) - z_-^2 R(z_-)}{z_+ - z_-} \right] \right\}, \quad (4.1b)$$

$$K_{12}(k) = -K_{21}(k) = -i\eta \frac{\omega_p^2}{\omega^2} \frac{y}{1+y^2} \left[ \frac{(z-z_+)S(z_+) - (z-z_-)S(z_-)}{z_+ - z_-} \right], \quad (4.1c)$$

$$K_{13}(k) = K_{31}(k) = -\frac{\omega_p^2}{\omega^2} \frac{\tan \theta}{1+y^2} \left[ \frac{(z-z_+)z_+R(z_+) - (z-z_-)z_-R(z_-)}{z_+ - z_-} \right], \quad (4.1d)$$

$$K_{23}(k) = -K_{32}(k) = i\eta \frac{\omega_p^2}{\omega^2} \frac{y \tan \theta}{1+y^2} \left[ \frac{z_+S(z_+) - z_-S(z_-)}{z_+ - z_-} \right], \quad (4.1e)$$

with argument ( $k$ ) denoting the wave 4-vector  $(\omega, \mathbf{k})$ , and where  $\theta$  is the angle between  $\mathbf{k}$  and the ambient magnetic field. It is implicit that a summation over the contributions of electrons ( $\eta = -1$ ) and positrons ( $\eta = +1$ ) is performed. The number density  $n = n_+ + n_-$  in the definition (3.2) of the plasma frequency is summed over the number densities  $n_-$  and  $n_+$  of the electrons and positrons. After summing over the electrons and positrons,  $\eta$  in (4.1) may be interpreted as  $(n_+ - n_-)/n$ . The gyrotropic components are those proportion to  $\eta$ , and we neglect gyrotropy in the following discussion by assuming  $\eta = 0$ . A non-gyrotropic medium has  $K_{12}(k) = 0$  and  $K_{23}(k) = 0$ , in which case the natural waves modes have zero circular polarization.

#### 4.1. The low-frequency limit

Dispersion in a pulsar plasma has been investigated in detail (GMG; MGKF) in the low-frequency limit, which actually corresponds to retaining only the lowest-order terms in an expansion in  $\gamma(\omega - k_{\parallel}v)/\Omega_e$ . Formally, this corresponds to the limit of large  $y$ , with only terms up to order  $1/y^2$  retained in the expansion of (4.1) in powers of  $1/y$ . This expansion involves only the explicit  $y$ -dependence in (4.1), with  $y^2 \rightarrow \infty$  elsewhere implying, according to Table 1,  $z_{\pm} \rightarrow \pm 1$ . One has

$$R(\pm 1) = \mp \langle \gamma \rangle - \langle \gamma v \rangle, \quad S(\pm 1) = \mp 1 - \langle v \rangle. \quad (4.2)$$

In this paper, we consider only distributions that are reflection-symmetric,  $f(-p) = f(p)$ , implying  $\langle v \rangle = 0$  and  $\langle \gamma v \rangle = 0$ .

For the low-frequency limit to be valid, one requires that the parameter  $\gamma(\omega - k_{\parallel}v)/\Omega_e$  be small, and this corresponds to

$$\frac{(1+y^2)(v-z_+)(v-z_-)}{y^2(1-v^2)} \ll 0. \quad (4.3)$$

The condition (4.3) is satisfied provided that the important contributions to the dispersion come from particles with  $v$  well inside the ellipse defined by  $v = z_{\pm}$ ; cf. Fig. 2. The condition (4.3) is satisfied for  $y \gg 1$ ,  $z \ll y$ , which corresponds to the low-frequency limit, and also for  $z \rightarrow 1$  (implying  $z_{\pm} \rightarrow 1$ ) and  $y \gtrsim 1$ , that is, near the light line for frequencies  $\omega \lesssim \Omega_e$ .

## 5. Choice of distribution functions

For our numerical calculations, we choose two different distribution functions: a one-dimensional Jüttner distribution and a soft bell distribution. A Jüttner distribution is a (relativistically correct) thermal distribution, and in this case the RPDFs need to be evaluated by numerical integration. A bell-type distribution (GMG; MGKF) has the computational advantage that the RPDFs can be evaluated in terms of simple functions.

5.1. Jüttner distribution

A one-dimensional Jüttner distribution is

$$f(u) = \frac{e^{-\rho\gamma}}{2K_1(\rho)}, \tag{5.1}$$

where  $\rho = m/T$  is the inverse temperature in units of the rest energy and  $K_n$  is a modified Bessel (Macdonald) function of order  $n$  (Abramowitz and Stegun 1965). A plasma dispersion function for such a distribution is that defined by Godfrey et al. (1975):

$$T(z, \rho) = \int_{-1}^1 dv \frac{e^{-\rho\gamma}}{v - z}. \tag{5.2}$$

In terms of this function, the dispersion functions defined by (3.3) become

$$W(z) = \frac{T'(z, \rho)}{2K_1(\rho)}, \tag{5.3a}$$

$$R(z) = \frac{1}{2K_1(\rho)} \frac{\partial^2 T(z, \rho)}{\partial \rho^2}, \tag{5.3b}$$

$$S(z) = -\frac{1}{2K_1(\rho)} \frac{\partial T(z, \rho)}{\partial \rho}, \tag{5.3c}$$

with  $T'(z, \rho) = \partial T(z, \rho)/\partial z$ . Using the identities (Godfrey et al. 1975)

$$(1 - z^2) \frac{\partial^2}{\partial \rho^2} T(z, \rho) = 2zK_0(\rho) + T(z, \rho), \tag{5.4}$$

$$z \frac{\partial}{\partial \rho} T(z, \rho) = 2K_1(\rho) + \frac{(1 - z^2)}{\rho} T'(z, \rho), \tag{5.5}$$

(5.3b,c) become

$$R(z) = \frac{2z K_0(\rho) + T(z, \rho)}{(1 - z^2) 2K_1(\rho)}, \tag{5.6a}$$

$$S(z) = -\frac{1}{z} \left[ 1 + \frac{(1 - z^2)}{\rho} \frac{T'(z, \rho)}{2K_1(\rho)} \right]. \tag{5.6b}$$

Also, for a one-dimensional Jüttner distribution one has

$$\left\langle \frac{1}{\gamma} \right\rangle = \frac{K_0(\rho)}{K_1(\rho)}. \tag{5.7}$$

Polyakov (1983) introduced the function

$$J(\gamma_0) = \int_1^\infty \frac{d\gamma}{(\gamma^2 - 1)^{1/2}} \frac{e^{-\rho\gamma}}{\gamma + \gamma_0}. \tag{5.8}$$

The relation between this function and  $T(z, \rho)$  is

$$-z[J(\gamma_0) + J(-\gamma_0)] = \frac{\partial}{\partial \rho} T(z, \rho). \tag{5.9}$$

with  $\gamma_0 = (1 - z^2)^{-1/2}$  here, and where (5.5) is used.

5.2. Soft bell distribution

The bell-type distributions are of the form

$$f(u) \propto (u_m^2 - u^2)^n H(u_m^2 - u^2), \tag{5.10}$$

where  $u_m$  is an upper cutoff and  $H(x) = 0$  for  $x < 0$ ,  $H(x) = 1$  for  $x > 0$  is the step function. The cases  $n = 0, 1, 2, 3$  are the water bag, hard bell, soft bell and squishy bell distributions respectively. For many of our detailed calculations, we choose the soft bell distribution

$$f(u) = \frac{15}{16u_m^5} (\gamma_m^2 - \gamma^2)^2 H(u_m^2 - u^2). \quad (5.11)$$

It has the moments

$$\langle \gamma \rangle = \frac{5}{128u_m^5} [u_m(1 + u_m^2)^{1/2}(8u_m^4 - 10u_m^2 - 3) + 3(8u_m^4 + 4u_m^2 + 1) \sinh^{-1} u_m], \quad (5.12a)$$

$$\left\langle \frac{1}{\gamma} \right\rangle = \frac{15(1 - v_m^2)^{1/2}}{16v_m^5} \left[ \frac{3 + 2v_m^2 + 3v_m^4}{8} \ln \left| \frac{1 + v_m}{1 - v_m} \right| - \frac{3v_m}{4} (1 + v_m^2) \right]. \quad (5.12b)$$

The real and imaginary parts of the RPDFs used below are

$$\begin{aligned} W(z) &= \frac{15(1 - v_m^2)^{1/2}}{32v_m^5(1 - z^2)} \left[ 4v_m - \frac{2v_m}{(1 - z^2)} (1 - 5z^2 + 3v_m^2 + z^2v_m^2) \right. \\ &\quad \left. + (3z^4 + 6z^2 - 1 + v_m^2z^4 - 3v_m^2 - 6v_m^2z^2) \frac{(1 - v_m^2)}{(1 - z^2)^2} \ln \left| \frac{1 + v_m}{1 - v_m} \right| \right. \\ &\quad \left. + \frac{8z(1 - v_m^2)(v_m^2 - z^2)}{(1 - z^2)^2} \ln \left| \frac{v_m + z}{v_m - z} \right| \right] - i\pi \frac{15z(\gamma_m^2 - \gamma_0^2)}{4u_m^5(1 - z^2)^2} H(v_m - z), \quad (5.13) \\ R(z) &= \frac{15(1 - v_m^2)^{1/2}}{128v_m^5(1 - z^2)^3} \left\{ -2zv_m[(7v_m^2 - 1) - 2z^2(1 + 5v_m^2) + 3z^4(1 + v_m^2)] \right. \\ &\quad \left. + z[v_m^4(15 - 10z^2 + 3z^4) - v_m^2(6 + 12z^2 - 2z^4) \right. \\ &\quad \left. - 1 + 3z^4 + 6z^2] \ln \left| \frac{1 + v_m}{1 - v_m} \right| - 8(v_m^2 - z^2)^2 \ln \left| \frac{v_m + z}{v_m - z} \right| \right\} \\ &\quad + i\pi \frac{15\gamma_0^3}{16v_m^5\gamma_m} (v_m^2 - z^2)^2 H(v_m - z). \quad (5.14) \end{aligned}$$

The expression for  $W(z)$  corrects the expression found in GMG (their equation (62)).

### 5.3. Properties of $R(z)$

The properties of the function  $R(z)$  are illustrated in Figs 3–6. In Figs 3 and 4, the function  $z^2R(z)$  is compared with  $z^2W(z)$  for a Jüttner distribution and for a soft bell distribution respectively, each for two different values of  $\langle \gamma \rangle$ . It is apparent that  $z^2R(z)$  differs from  $z^2W(z)$  in (a) being predominantly negative, (b) smaller in magnitude and (c) less sharply peaked. In Fig. 5,  $R(z)$  is shown for a Jüttner distribution ranging from non-relativistic,  $\rho = 15$ , to significantly relativistic,  $\rho = 0.5$ . The function  $R(z)$  is similar to  $T(z, \rho)$ ; specifically, in the non-relativistic limit,  $\rho \gg 1$ , one has  $R(z) \approx T(z, \rho)$ . As with the functions  $T(z, \rho)$  (MGKF),  $R(z)$  develops a sharp (negative) peak that sharpens and moves closer to  $z = 1$  as  $\rho \lesssim 1$  decreases. The properties of  $R(z)$  are of interest only for  $-1 \leq z \leq 1$ , owing to the arguments  $z_{\pm}$  in (4.1) being restricted to this range. The peak occurs at about the mean thermal speed. In Fig. 6, the function  $R(z)$  is compared for Jüttner, soft bell and squishy bell distributions; the function is the least strongly peaked for the Jüttner distribution.

A feature of  $R(z)$  that has no counterpart for  $T(z, \rho)$  is that, for sufficiently small  $z$ , the function changes sign as  $\rho$  decreases. This sign change occurs at  $\rho \approx$

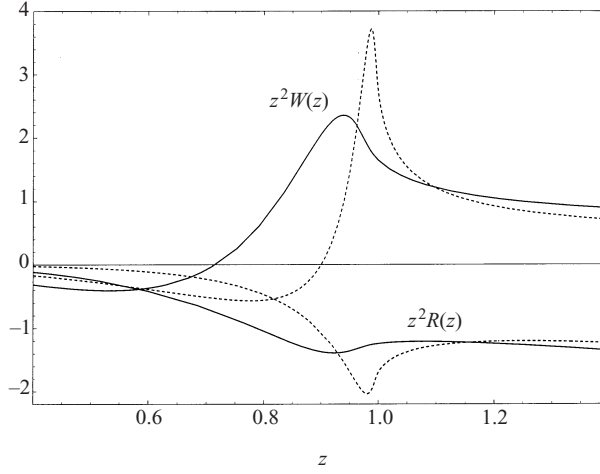


**Figure 3.** Plots of  $z^2 R(z)$  and  $z^2 W(z)$  for a Jüttner distribution with  $\rho = 1$  (dotted) and 2.5 (solid).

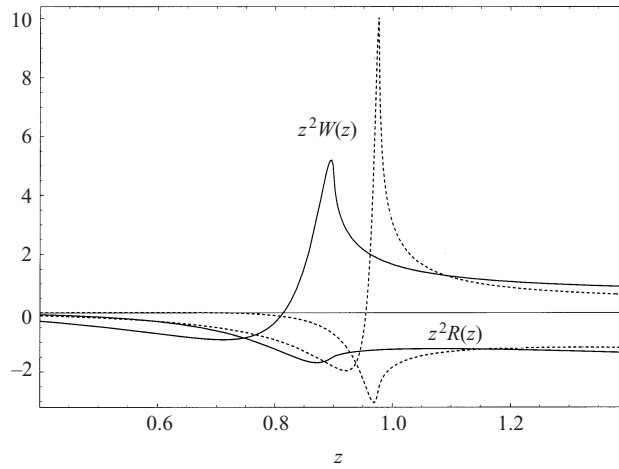


**Figure 4.** Plots of  $z^2 R(z)$  and  $z^2 W(z)$  for a soft bell distribution with  $v_m = 0.977098$  (dotted) and 0.9 (solid).

0.496. This value may be determined analytically for the Jüttner distribution by expanding the relation (5.6) for  $R(z)$  by using the expansion of  $T(z, \rho)$  in powers of  $z$ ; the linear term is  $z[K_0(\rho) - Ki_2(\rho)]/K_1(\rho)$ , where  $Ki_n(\rho)$  is the  $n$ th integral of  $K_0$  (Abramowitz and Stegun 1965), and this is negative for large  $\rho$  and positive for small  $\rho$ . For bell distributions, there is an analogous change in sign of the small- $z$  limit of  $R(z)$  for  $u_m \approx 2$ . The specific functions that appear in the response tensor are  $R(z_{\pm})$ , and hence this small-argument feature is relevant for small  $z_{\pm}$  (cf. Table 1).

## 6. Dispersion curves

The properties of waves in a pulsar plasma have been investigated in detail (GMG; MGKF) only for a non-gyrotropic plasma in the low-frequency limit with  $v_A \gg 1$ . Relaxing these restrictions leads to a rich variety of additional features, some

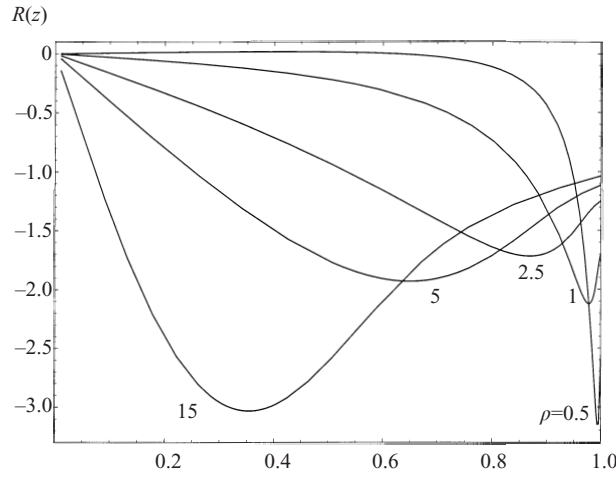


**Figure 5.** Plot of  $R(z)$  for the Jüttner distribution with  $\rho = 0.5, 1, 2.5, 5$  and  $15$ .

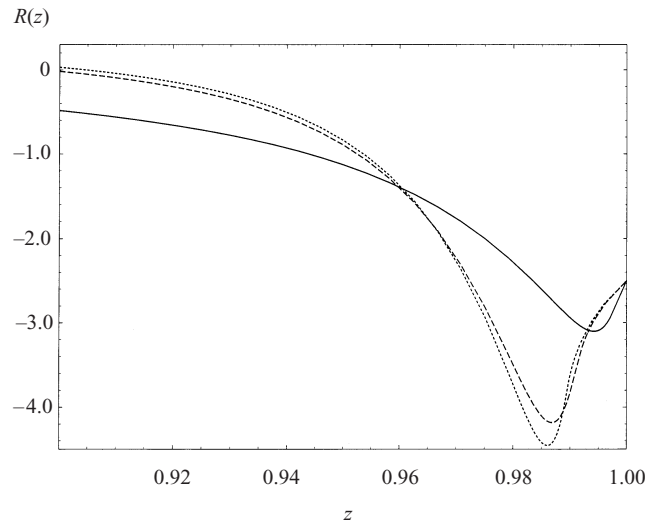


**Figure 6.** Plot of  $R(z)$  for three different distributions with  $\langle \gamma \rangle = 2.5$ . The solid, dashed and dotted curves correspond respectively to the Jüttner, squishy and soft bell distributions.

of which are outlined here. We consider only the non-gyrotropic case, and then the dispersion equation factors into two equations (GMG; MGKF) — one for the X mode (also called the  $t$  mode and the magnetoacoustic mode) and another that describes the Langmuir mode, the O mode and the Alfvén mode. The X mode has its electric vector along  $\mathbf{k} \times \mathbf{B}$ , and the other two modes have mixed longitudinal–transverse polarization in the  $(\mathbf{k}, \mathbf{B})$  plane.

## 6.1. X mode

The dispersion equation for the X mode is  $n^2 = K_{22}(k)$ , with the square of the refractive index written as  $n^2 = 1/z^2 \cos^2 \theta$  here. Then (4.1) gives

$$\frac{1}{z^2 \cos^2 \theta} = 1 - \frac{\omega_p^2}{\omega^2} \frac{1}{1+y^2} \left[ \left\langle \frac{1}{\gamma} \right\rangle + \frac{(z-z_+)^2 R(z_+) - (z-z_-)^2 R(z_-)}{z_+ - z_-} \right]. \quad (6.1)$$

In the low-frequency limit, (6.1) with (4.2) gives the dispersion relation

$$z^2 = \frac{v_A^2 - \tilde{v}^2 \cos^2 \theta}{(1+v_A^2) \cos^2 \theta}, \quad (6.2)$$

with  $\langle \gamma^{-1} \rangle = \langle \gamma \rangle (1 - \tilde{v}^2)$ . In a pulsar plasma, one expects  $v_A^2 \gg 1$ , and we concentrate on this case. However, before doing so, it is appropriate to note two features that apply for  $v_A^2 \lesssim 1$ . First, as is evident from (6.2), for  $v_A^2 \lesssim \tilde{v}^2$ , the solutions for  $z^2$  become negative, corresponding to the firehose instability (Gedalin 1993; GMG). The threshold for this instability corresponds to a solution with  $\omega = 0$  and  $k_{\parallel} \neq 0$ . Secondly, if one looks for a cutoff, corresponding to  $z^2 = \infty$  and  $\omega = \omega_c$  and  $k_{\parallel} = 0$ , then (6.1) reduces to

$$R \left( \left( 1 - \frac{\omega_c^2}{\Omega_e^2} \right)^{1/2} \right) = v_A^2 \langle \gamma \rangle \left( 1 - \frac{\omega_c^2}{\Omega_e^2} \right)^{1/2}. \quad (6.3)$$

With  $R(1) = \langle \gamma \rangle$ , it follows that a cutoff can occur at  $\omega_c \ll \Omega_e$  for  $v_A^2 \lesssim 1$ . The existence of such a cutoff suggests the appearance of a new mode. However, we do not discuss these small- $v_A$  features further in the present paper.

For  $v_A^2 \gg 1$ , with  $\tilde{v}^2 < 1$ , (6.2) implies that the X mode at low frequency is magnetoacoustic in character. The parallel phase speed  $z$  is less than unity at small angles of propagation,  $\sin^2 \theta < (1 + \tilde{v}^2)/v_A^2$ , and is greater than unity when this inequality is reversed. At sufficiently high frequencies, all waves in a plasma have phase speed greater than unity, and hence the dispersion curve for small  $\theta$  must cross the light line,  $z = 1$ , at least once.

For high Alfvén speeds, we identify three classes of dispersion curves for the X mode at fixed  $\theta$ . The first class has  $z < 1$  at low frequencies and crosses the light line once, the second class has  $z > 1$  at low frequencies and crosses the light line twice, and the third class is always in the region  $z > 1$ . These three classes correspond to small angles, a narrow intermediate range of angles and large angles respectively, with the values of the angles that separate these regimes depending on the value of  $v_A$ . Examples of X-mode dispersion curves are shown in Fig. 7.

Any crossing of the light line defines a crossover frequency,  $\omega_{co}$ . To determine the crossover frequencies, one sets  $z = 1$ ,  $y = y_{co} = \Omega_e/\omega_{co}$ , in (6.1). This gives

$$\tan^2 \theta + \frac{1}{\langle \gamma \rangle v_A^2} \frac{y_{co}^2}{1+y_{co}^2} \left[ \left\langle \frac{1}{\gamma} \right\rangle - \frac{2y_{co}^2}{1+y_{co}^2} R \left( \frac{1-y_{co}^2}{1+y_{co}^2} \right) \right] = 0. \quad (6.4)$$

With  $R(z) = -R(-z)$  negative for  $z > 0$  (an exception being for small  $z$  in a highly relativistic plasma), (6.4) has a solution only for  $y_{co}^2 > 1$ , corresponding to  $\omega_{co} < \Omega_e$ . In Fig. 8, the solution of (6.4) for  $\omega_{co}/(\Omega_e/\langle \gamma \rangle)$  is plotted as a function of  $\Omega_e/\omega_p$  for a range of angles  $0 \leq \theta \leq 1$ . For a given  $\theta$ , the curve defined by (6.4) has a nearly horizontal portion at  $\omega_{co} \approx \Omega_e/\langle \gamma \rangle$ , a nose that defines the maximum value of  $\Omega_e/\omega_p$ , and a nearly vertical portion at  $\Omega_e/\omega_p = [\langle \gamma \rangle (1 + \tilde{v}^2)]^{1/2} / \tan \theta$ . For fixed  $\theta$  and  $\Omega_e/\omega_p$ , a solution is defined by the intersection of the curves for that  $\theta$  with

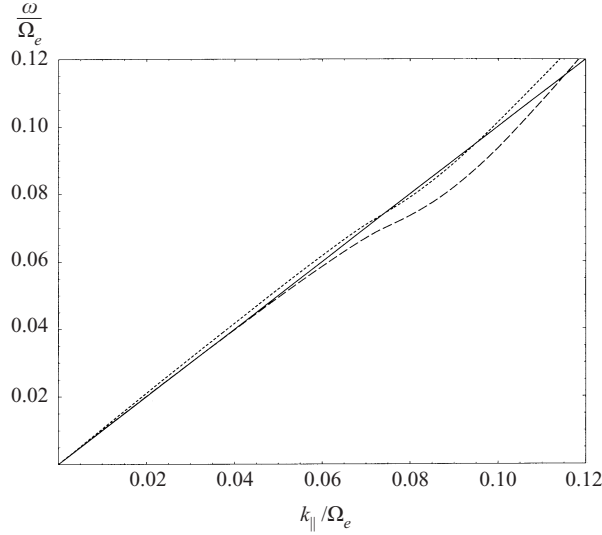


**Figure 7.** Dispersion relation of the X mode with  $\theta = 0$ ,  $\Omega_e/\omega_p = 5$  (dotted) and 4 (dashed) for a soft bell distribution with  $v_m = 0.9$ . The straight line is the light line,  $\omega = k_{\parallel}$ .

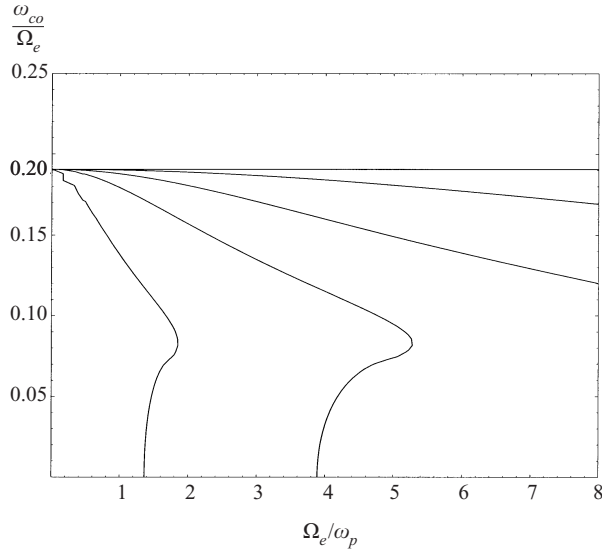


**Figure 8.**  $\omega_{co}/\Omega_e$  versus  $\Omega_e/\omega_p$  for the X mode with  $\theta = 0, 0.1, 0.25, 0.5$  and 1 for the soft bell distribution with  $v_m = 0.99$ . The horizontal line corresponds to  $\theta = 0$ , and as  $\theta$  increases, the curve becomes more curved.

a vertical line at that value of  $\Omega_e/\omega_p$ , with this value decreasing as  $\theta$  increases. It is apparent that for  $\Omega_e/\omega_p$  to the left of the vertical portion of the curve, there is one crossing, there are two crossings for an intermediate range of angles between the vertical portion and the nose, and no crossings for  $\Omega_e/\omega_p$  to the right of the nose. These crossovers occur at  $\omega_{co} \lesssim \Omega_e/\langle\gamma\rangle$ , that is, below about the mean relativistic gyrofrequency. At higher frequencies the dispersion curve for the X mode is entirely in the superluminal range,  $z > 1$ , for all angles of propagation.

Our results may be compared with analytic approximations obtained by Polyakov (1997), who considered dispersion in a highly relativistic electron–positron plasma with a Jüttner distribution. Polyakov found a solution for crossover frequencies in the ultrarelativistic limit. To relate our notation to Polyakov’s, it is convenient to write  $\gamma_{\pm} = (1 - z_{\pm}^2)^{-1/2}$ , and then  $z \rightarrow 1$  implies  $\gamma_+ \rightarrow \infty$  and  $\gamma_- \rightarrow (1 + y^2)/2y$ . Polyakov’s analytic solution for the crossover corresponds to  $\rho\gamma_- = x_0$ , with  $x_0 = 0.88$ , which leads to two solutions

$$\omega = \frac{\rho\Omega_e}{2x_0}, \quad \omega = \frac{2x_0\Omega_e}{\rho}, \quad (6.5a,b)$$

which Polyakov interpreted as two new wave modes. The first of the frequencies (6.5) is consistent with our results if it is interpreted as the crossover frequency for parallel propagation (for a highly relativistic Jüttner distribution). The second of the frequencies (6.5) corresponds to  $y_{co} \ll 1$  and is inconsistent with our analysis, which implies no solutions of (6.4) with  $y_{co} < 1$  for parallel propagation. We note that Polyakov’s analysis involves only  $v^2$ , rather than  $v$ , and that it allows a spurious resonance at  $v = -z_-$  for  $z = 1$ , in addition to the only physical resonance at  $v = z_-$  in this case. We suggest that the solution (6.5b) is unphysical and is associated with this spurious resonance.

## 6.2. The Langmuir and Alfvén modes

For parallel propagation, the dispersion equations for the Langmuir and Alfvén modes are independent of each other, and the two modes are independent except where their dispersion curves intersect. For oblique propagation in the low-frequency limit with  $v_A^2 \gg 1$ , the Langmuir and Alfvén modes reconnect, with the reconnected dispersion curves both deviating away from the intersection point for  $\theta = 0$ , to form the oblique Alfvén mode and the L–O mode (GMG; MGKF). For sufficiently large  $v_A^2$  only the L–O mode extends to higher frequencies, and it is the only mode to be significantly modified by the cyclotron resonance. Before discussing the L–O mode, it is appropriate to comment on the other modes.

The dispersion of the parallel Langmuir mode is independent of  $\Omega_e$ , and hence is the same as in the low-frequency case, cf. MGKF. Examples of dispersion curves are illustrated in Fig. 9 for a weakly relativistic case to illustrate the dependence on the choice of distribution function. The differences occur at lower values of  $z$ , where Landau damping is relatively strong, so that the differences evident in Fig. 9 are of relatively little physical significance. As the particles become more highly relativistic, the ratio of the frequencies where the Langmuir mode crosses the light line to that where it cuts off increases proportionally to  $\langle\gamma\rangle$ . The highest frequency of the Langmuir mode, of the order of  $\omega_p\langle\gamma\rangle^{1/2}$ , is below the cyclotron resonance for  $v_A \gtrsim \langle\gamma\rangle$ , and we concentrate on this case in the following discussion.

The dispersion of the parallel Alfvén mode is the same as that for the parallel X mode. It follows that for the parallel Alfvén mode, there is one crossover frequency, which is determined by the curve for  $\theta = 0$  in Fig. 8.

For  $v_A \gtrsim \langle\gamma\rangle \gg 1$ , the oblique Alfvén mode is restricted to frequencies  $\lesssim \omega_p\langle\gamma\rangle^{1/2}$ , and the low-frequency approximation (GMG; MGKF) adequately describes its properties. For smaller  $v_A^2$ , and specifically for  $v_A^2 \lesssim 1$ , the properties of the oblique Alfvén mode are modified in similar ways to the X mode for  $v_A^2 \lesssim 1$ , but we do not discuss this limit in detail in this paper.

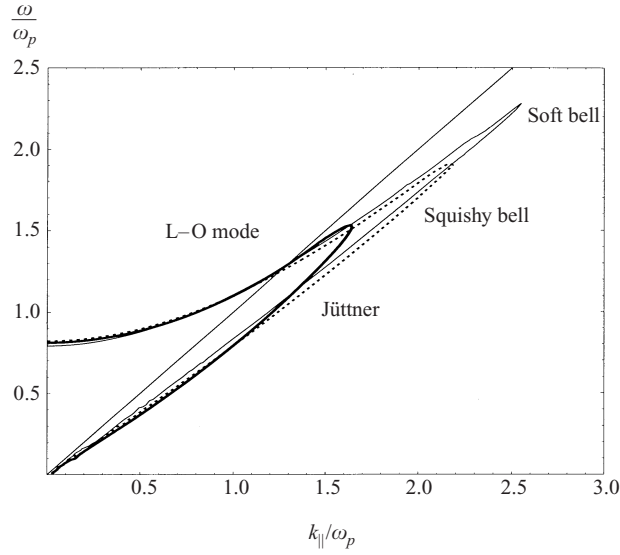


**Figure 9.** Dispersion relations of the L–O mode with  $\theta = 0$  and  $\Omega_e/\omega_p = 10$  for three different distribution functions: soft bell (thin solid line); squishy bell (dotted line); Jüttner (thick solid line). For the soft bell and squishy bell distributions, we assume  $v_m = 0.9$ , and for the Jüttner distribution,  $\rho = 2.5$ . With the chosen parameters, both the soft bell and Jüttner distributions give  $\langle\gamma\rangle \approx 1.24$ , while the squishy bell distribution gives  $\langle\gamma\rangle \approx 1.2$ . The straight line is the light line,  $\omega = k_{\parallel}$ .

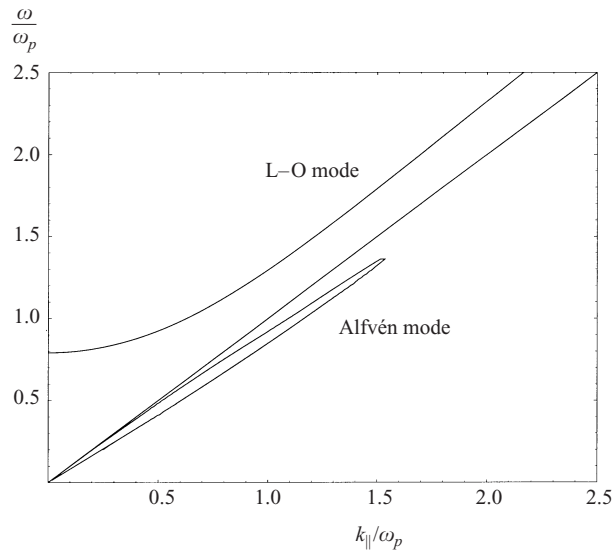


**Figure 10.** Dispersion relations of the L mode and the Alfvén mode with  $\theta = 0.5$  and  $\Omega_e/\omega_p = 10$  for a soft bell distribution with  $v_m = 0.9$ . The straight line is the light line,  $\omega = k_{\parallel}$ .

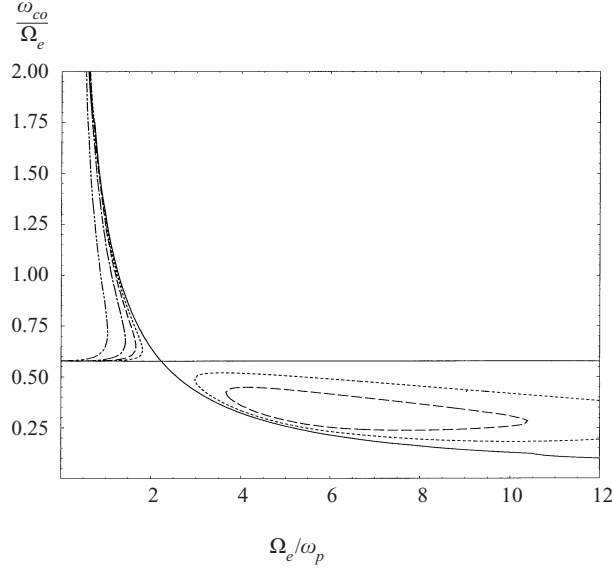


**Figure 11.**  $\omega_{co}/\Omega_e$  versus  $\Omega_e/\omega_p$  for the L–O mode with  $\theta = 0, 0.1, 0.15, 0.25$  and  $0.5$  for the soft bell distribution with  $v_m = 0.9$ .

The L–O mode extends to high frequencies (cf. Fig. 10). As in our discussion of the X mode, the main emphasis here is on the existence of a region where the L–O mode has  $z < 1$ . The condition for the dispersion curve to cross the light line is

$$\begin{aligned}
 (1 - z_{co}) \left[ \left\langle \frac{1}{\gamma} \right\rangle - (1 - z_{co})R(z_{co}) \right] & \left\{ 2(1 - \tan^2 \theta) \frac{\Omega_e^2}{\omega_p^2} - 2y_{co}^2 W(1) \right. \\
 & \left. - \tan^2 \theta \left[ (1 - z_{co}) \left\langle \frac{1}{\gamma} \right\rangle + R(1) - z_{co}^2 R(z_{co}) \right] \right\} \\
 & + \tan^2 \theta \left\{ 2 \frac{\Omega_e^2}{\omega_p^2} + (1 - z_{co}) \left[ \left\langle \frac{1}{\gamma} \right\rangle + z_{co} R(z_{co}) \right] \right\}^2 = 0, \quad (6.6)
 \end{aligned}$$

with  $z_{co} = (1 - y_{co}^2)/(1 + y_{co}^2)$ . Solutions of (6.6) are plotted in Fig. 11. For  $\theta = 0$ , there are two crossovers, one for the parallel Langmuir mode, at  $\omega_{co} = \omega_p [\langle \gamma \rangle (1 + \tilde{v}^2)]^{1/2}$ , and one that is the same as for the parallel X mode. For  $\Omega_e \gg \omega_p$ , the crossover for the Alfvén mode, which is the horizontal line for  $\theta = 0$  in Fig. 11, is at a much higher frequency than the Langmuir mode crossover. The L–O mode is subluminal between these frequencies. As  $\theta$  increases, the two crossover frequencies approach each other, becoming equal at some  $\theta_{\max}$ , with the L–O mode having no subluminal portion for  $\theta > \theta_{\max}$ . The righthand limit of the closed curve in Fig. 11 defines  $\theta_{\max}$  for a given  $\Omega_e/\omega_p$ . The curves on the left in Fig. 11 apply when the crossover for the parallel Langmuir mode is at a higher frequency than that for the Alfvén mode, and we do not discuss this case here.

## 7. Discussion and conclusions

The inclusion of the cyclotron resonance in the theory of dispersion in an intrinsically relativistic, one-dimensional pair plasma involves three RPDFs:  $W(z)$ , which describes the dispersion associated with the Landau resonance,  $v = z$ , and  $R(z_{\pm})$

and  $S(z_{\pm})$ , which describe the dispersion associated with the normal and anomalous Doppler resonances,  $v = z_{\pm}$ . These two cyclotron resonances are given by (2.3), and are illustrated in Fig. 2. The RPDFs  $R(z_{\pm})$  and  $S(z_{\pm})$  apply to the non-gyrotropic and gyrotropic parts of the response respectively. Only the non-gyrotropic case is discussed in detail in this paper. The RPDF  $R(z)$  is evaluated in Sec. 5 for bell-type distributions and for a Jüttner distribution.

In discussing wave dispersion, we consider only the non-gyrotropic case, and concentrate on the limit  $v_A \gg 1$ . Main interest here is centred around how the known dispersion curves at low frequencies connect to high frequencies across the cyclotron resonance. A specific interest is in the parameters for which the waves are subluminal in the sense that  $z < 1$ : the only possible kinetic instabilities, leading to growth of wave in a pulsar plasma, are at the Landau and anomalous cyclotron resonances, both of which require  $z < 1$ . In all cases considered here, the value of  $z$  increases as the angle of propagation,  $\theta$ , increases, and dispersion with  $z < 1$  is restricted to sufficiently small angles. For the X mode, there can be zero, one or two crossings of  $z = 1$ . At very small angles of propagation, the dispersion curve has  $z < 1$  at low frequencies, and it crosses  $z = 1$  at a crossover frequency  $\omega_{co} \sim \Omega_e / \langle \gamma \rangle$ . As  $\theta$  increases, the value of  $z$  at low frequencies increases from  $z < 1$  to  $z > 1$ . There is a small range of angles for which the dispersion curve has  $z > 1$  at low frequencies and crosses  $z = 1$  twice near  $\Omega_e / \langle \gamma \rangle$ . For larger  $\theta$ , the dispersion curve is confined to  $z > 1$ . For the L–O mode, there can be zero or two crossings. The main qualitative difference from the X mode is at low frequency. The L–O mode is Langmuir-like for  $\omega \lesssim \omega_p \langle \gamma \rangle^{1/2}$ , where it has  $z > 1$ . For  $\theta \rightarrow 0$ , this dispersion crosses  $z = 1$  at  $\omega = \omega_p [\langle \gamma \rangle (1 + \tilde{v}^2)]^{1/2}$ , and it recrosses  $z = 1$  at the same frequency as for the X mode for  $\theta = 0$ . As  $\theta$  increases, these two crossover frequencies approach each other, and above the angle at which they coincide, the L–O mode is entirely superluminal.

Wave modes for  $\theta = 0$  were discussed by Polyakov (1997), and our results for the higher-frequency crossing of  $z = 1$  are consistent with the higher frequency of Polyakov’s solutions, which he interpreted as defining two new modes. We suggest that the other of Polyakov’s solutions is spurious.

There is a rich variety of features of the wave dispersion that we are currently investigating. Features for which we have preliminary results (Kennett 2000) include additional branches of the X mode and the Alfvén mode for  $v_A \lesssim 1$ , one of which is associated with the firehose instability, and the damping of the waves due to the normal Doppler resonance and their growth due to the anomalous Doppler resonance. All of our preliminary results apply to the non-gyrotropic case, and an important generalization that we have yet to investigate is to include non-zero charge and current densities, leading to non-zero gyrotropic components  $K_{12} = -K_{21}$  and  $K_{23} = -K_{32}$  respectively. This generalization is necessary in order to discuss the circular polarization of the wave modes and its possible effect on the observed circular polarization of pulsar radio emission. The general theory presented in this paper is needed to discuss all of these effects.

## Appendix. Derivation of the response tensor

The covariant expression for the response tensor for an arbitrary distribution  $F(p)$  in 8-dimensional  $(x, p)$  space of particles of one species with mass  $m$  and charge  $q$

is (Melrose 1997)

$$\alpha^{\mu\nu}(k) = -\frac{q^2}{m} \int d^4p F(p) \sum_{s=-\infty}^{\infty} G^{\alpha\mu}(s, k, u) \tau_{\alpha\beta}((ku)_{\parallel} - s\Omega_e) G^{*\beta\nu}(s, k, u), \quad (\text{A } 1)$$

$$\tau^{\mu\nu}(\omega) = g_{\parallel}^{\mu\nu} + \frac{\omega}{\omega^2 - \Omega_e^2} (\omega g_{\perp}^{\mu\nu} + i\eta \Omega_e f^{\mu\nu}), \quad (\text{A } 2)$$

$$G^{\mu\nu}(s, k, u) = g^{\mu\nu} J_s(k_{\perp} R) - \frac{k^{\mu} U^{\nu}(s, k)}{(ku)_{\parallel} - s\Omega_e}, \quad (\text{A } 3)$$

$$U^{\mu}(s, k) = (\gamma J_s(k_{\perp} R), \gamma \mathbf{V}(s, k)), \quad (\text{A } 4)$$

$$\begin{aligned} \mathbf{V}(s, k) = & \left( \frac{1}{2} v_{\perp} [e^{-i\eta\psi} J_{s-1}(k_{\perp} R) + e^{i\eta\psi} J_{s+1}(k_{\perp} R)] \right. \\ & \left. - \frac{1}{2} i\eta v_{\perp} [e^{-i\eta\psi} J_{s-1}(k_{\perp} R) - e^{i\eta\psi} J_{s+1}(k_{\perp} R)], v_{\parallel} J_s(k_{\perp} R) \right), \end{aligned} \quad (\text{A } 5)$$

with  $\Omega_e = |q|B/m$ ,  $\eta = q/|q|$  and  $R = \gamma v_{\perp}/\Omega_e$ . We consider a one-dimensional distribution in which all the particles have  $v_{\perp} = 0$ . Then one has  $R = \gamma v_{\perp}/\Omega_e = 0$ , and hence the argument  $k_{\perp} R$  of the Bessel function is zero, implying  $J_s(0) = 0$  for  $s \neq 0$ , and  $J_0(0) = 1$  implies that only the term  $s = 0$  remains in the sum in (A 5), giving

$$G^{\alpha\mu}(0, k, u) \tau_{\alpha\beta}((ku)_{\parallel}) G^{*\beta\nu}(0, k, u) = G^{\alpha\mu}(k, u_{\parallel}) \tau_{\alpha\beta}((ku)_{\parallel}) G^{\beta\nu}(k, u_{\parallel}), \quad (\text{A } 6)$$

with

$$G^{\mu\nu}(k, u_{\parallel}) = g^{\mu\nu} - \frac{k^{\mu} u_{\parallel}^{\nu}}{k u_{\parallel}}. \quad (\text{A } 7)$$

The subscript  $\parallel$  is omitted below.

We are free to choose a coordinate system in which  $\mathbf{k}$  is in the 1–3 plane, so that we have  $k^{\mu} = (\omega, k_{\perp}, 0, k_{\parallel})$ . Then one may introduce the 4-vectors

$$k_{\parallel}^{\mu} = g_{\parallel}^{\mu\nu} k_{\nu} = (\omega, 0, 0, k_{\parallel}), \quad k_{\perp}^{\mu} = g_{\perp}^{\mu\nu} k_{\nu} = (0, k_{\perp}, 0, 0), \quad (\text{A } 8a, b)$$

$$\tilde{k}_{\perp}^{\mu} = -f^{\mu\nu} k_{\nu} = (0, 0, k_{\perp}, 0), \quad k_D^{\mu} = \phi^{\mu\nu} k_{\nu} = (k_{\parallel}, 0, 0, \omega). \quad (\text{A } 8c, d)$$

Then

$$\begin{aligned} \alpha^{\mu\nu}(k) = & -\frac{q^2}{m} \int d^4p F(p) \left\{ -\frac{k_D^{\mu} k_D^{\nu}}{(ku)^2} + \frac{(ku)^2}{(ku)^2 - \Omega_e^2} \left[ g_{\perp}^{\mu\nu} - \frac{k_{\perp}^{\mu} u^{\nu} + k_{\perp}^{\nu} u^{\mu}}{ku} - \frac{k_{\perp}^2 u^{\mu} u^{\nu}}{(ku)^2} \right] \right. \\ & \left. + i\eta \frac{\Omega_e ku}{(ku)^2 - \Omega_e^2} \left[ f^{\mu\nu} + \frac{\tilde{k}_{\perp}^{\mu} u^{\nu} - \tilde{k}_{\perp}^{\nu} u^{\mu}}{ku} \right] \right\}. \end{aligned} \quad (\text{A } 9)$$

In evaluating (A 9), the 4-vectors (A 8) may be used to construct a set of basis vectors for the vacuum polarization tensor (Shabad 1975). In the presence of a plasma, it is convenient to introduce the 4-velocity  $\bar{u}^{\mu}$  of the rest frame of the plasma. The coordinate system used here corresponds to

$$\begin{aligned} e_0^{\mu} = \bar{u}^{\mu} = & (1, 0, 0, 0), \quad e_1^{\mu} = \frac{k_{\perp}^{\mu}}{k_{\perp}} = (0, 1, 0, 0), \\ e_2^{\mu} = \frac{\tilde{k}_{\perp}^{\mu}}{k_{\perp}} = & (0, 0, 1, 0), \quad e_3^{\mu} = \frac{k_{\parallel}^{\mu} - (k\bar{u})\bar{u}^{\mu}}{[(k\bar{u})^2 - k_{\parallel}^2]^{1/2}} = (0, 0, 0, 1). \end{aligned} \quad (\text{A } 10)$$

The following averages appear:

$$\left\langle \frac{1}{\gamma(ku)^2} \right\rangle = \frac{1}{k_{\parallel}^2} \left\langle \frac{1}{\gamma^3(v-z)^2} \right\rangle, \quad (\text{A 11a})$$

$$\left\langle \frac{(ku)^2}{\gamma[(ku)^2 - \Omega_e^2]} \right\rangle = \frac{1}{1+y^2} \left\langle \frac{(v-z)^2}{\gamma(v-z_+)(v-z_-)} \right\rangle, \quad (\text{A 11b})$$

$$\left\langle \frac{ku}{\gamma[(ku)^2 - \Omega_e^2]} \right\rangle = -\frac{1}{k_{\parallel}(1+y^2)} \left\langle \frac{v-z}{\gamma(v-z_+)(v-z_-)} \right\rangle, \quad (\text{A 11c})$$

$$\left\langle \frac{u^\mu}{\gamma[(ku)^2 - \Omega_e^2]} \right\rangle = \frac{1}{k_{\parallel}^2(1+y^2)} \left\langle \frac{e_0^\mu + ve_3^\mu}{\gamma(v-z_+)(v-z_-)} \right\rangle, \quad (\text{A 11d})$$

$$\left\langle \frac{ku u^\mu}{\gamma[(ku)^2 - \Omega_e^2]} \right\rangle = -\frac{1}{k_{\parallel}(1+y^2)} \left\langle \frac{(v-z)(e_0^\mu + ve_3^\mu)}{\gamma(v-z_+)(v-z_-)} \right\rangle, \quad (\text{A 11e})$$

$$\left\langle \frac{u^\mu u^\nu}{\gamma[(ku)^2 - \Omega_e^2]} \right\rangle = \frac{1}{k_{\parallel}^2(1+y^2)} \left\langle \frac{e_0^\mu e_0^\nu + v(e_0^\mu e_3^\nu + e_0^\nu e_3^\mu) + v^2 e_3^\mu e_3^\nu}{\gamma(v-z_+)(v-z_-)} \right\rangle. \quad (\text{A 11f})$$

To reduce these to forms that involve only one resonant denominator, one uses

$$\frac{1}{(v-z_+)(v-z_-)} = \frac{1}{z_+ - z_-} \left( \frac{1}{v-z_+} - \frac{1}{v-z_-} \right), \quad (\text{A 12a})$$

$$\frac{v}{(v-z_+)(v-z_-)} = \frac{1}{z_+ - z_-} \left( \frac{z_+}{v-z_+} - \frac{z_-}{v-z_-} \right), \quad (\text{A 12b})$$

$$\frac{v^2}{(v-z_+)(v-z_-)} = 1 + \frac{1}{z_+ - z_-} \left( \frac{z_+^2}{v-z_+} - \frac{z_-^2}{v-z_-} \right). \quad (\text{A 12c})$$

Then, using (3.3), (A 11) reduce to

$$\left\langle \frac{1}{\gamma(ku)^2} \right\rangle = \frac{1}{k_{\parallel}^2} W(z), \quad (\text{A 13a})$$

$$\left\langle \frac{(ku)^2}{\gamma[(ku)^2 - \Omega_e^2]} \right\rangle = \frac{1}{1+y^2} \left[ \left\langle \frac{1}{\gamma} \right\rangle + \frac{(z-z_+)^2 R(z_+) - (z-z_-)^2 R(z_-)}{z_+ - z_-} \right], \quad (\text{A 13b})$$

$$\left\langle \frac{ku}{\gamma[(ku)^2 - \Omega_e^2]} \right\rangle = \frac{(z-z_+)S(z_+) - (z-z_-)S(z_-)}{k_{\parallel}(1+y^2)(z_+ - z_-)}, \quad (\text{A 13c})$$

$$\left\langle \frac{u^\mu}{\gamma[(ku)^2 - \Omega_e^2]} \right\rangle = \frac{[S(z_+) - S(z_-)]e_0^\mu + [z_+S(z_+) - z_-S(z_-)]e_3^\mu}{k_{\parallel}^2(1+y^2)(z_+ - z_-)}, \quad (\text{A 13d})$$

$$\begin{aligned} \left\langle \frac{ku u^\mu}{\gamma[(ku)^2 - \Omega_e^2]} \right\rangle &= \frac{(z-z_+)R(z_+) - (z-z_-)R(z_-)}{k_{\parallel}(1+y^2)(z_+ - z_-)} e_0^\mu \\ &\quad + \frac{(z-z_+)z_+R(z_+) - (z-z_-)z_-R(z_-)}{k_{\parallel}(1+y^2)(z_+ - z_-)} e_3^\mu, \end{aligned} \quad (\text{A 13e})$$

$$\begin{aligned} \left\langle \frac{u^\mu u^\nu}{\gamma[(ku)^2 - \Omega_e^2]} \right\rangle &= \frac{1}{k_{\parallel}^2(1+y^2)(z_+ - z_-)} \left\{ [R(z_+) - R(z_-)]e_0^\mu e_0^\nu \right. \\ &\quad \left. + [z_+R(z_+) - z_-R(z_-)](e_0^\mu e_3^\nu + e_0^\nu e_3^\mu) \right. \\ &\quad \left. + \left[ \left\langle \frac{1}{\gamma} \right\rangle + z_+^2 R(z_+) - z_-^2 R(z_-) \right] e_3^\mu e_3^\nu \right\}. \end{aligned} \quad (\text{A 13f})$$

The resulting specific expressions for the components of the response tensor are

$$\alpha^{00}(k) = \frac{q^2 n}{m} \frac{1}{1+y^2} \left[ W(z) + \frac{k_{\perp}^2}{k_{\parallel}^2} \frac{1}{1+y^2} \frac{R(z_+) - R(z_-)}{z_+ - z_-} \right], \quad (\text{A 14a})$$

$$\alpha^{01}(k) = \alpha^{10}(k) = \frac{q^2 n}{m} \frac{1}{1+y^2} \frac{k_{\perp}}{k_{\parallel}} \left[ \frac{(z - z_+)R(z_+) - (z - z_-)R(z_-)}{z_+ - z_-} \right], \quad (\text{A 14b})$$

$$\alpha^{02}(k) = -\alpha^{20}(k) = i\eta \frac{q^2 n}{m} \frac{1}{1+y^2} \frac{k_{\perp}}{k_{\parallel}} \left[ \frac{S(z_+) - S(z_-)}{z_+ - z_-} \right], \quad (\text{A 14c})$$

$$\alpha^{03}(k) = \alpha^{30}(k) = \frac{q^2 n}{m} \frac{1}{1+y^2} \left[ zW(z) + \frac{k_{\perp}^2}{k_{\parallel}^2} \frac{1}{1+y^2} \frac{z_+R(z_+) - z_-R(z_-)}{z_+ - z_-} \right], \quad (\text{A 14d})$$

$$\alpha^{11}(k) = \alpha^{22}(k) = \frac{q^2 n}{m} \frac{1}{1+y^2} \left[ \left\langle \frac{1}{\gamma} \right\rangle + \frac{(z - z_+)^2 R(z_+) - (z - z_-)^2 R(z_-)}{z_+ - z_-} \right], \quad (\text{A 14e})$$

$$\alpha^{33}(k) = \frac{q^2 n}{m} \left\{ z^2 W(z) + \frac{k_{\perp}^2}{k_{\parallel}^2} \frac{1}{1+y^2} \left[ \left\langle \frac{1}{\gamma} \right\rangle + \frac{z_+^2 R(z_+) - z_-^2 R(z_-)}{z_+ - z_-} \right] \right\}, \quad (\text{A 14f})$$

$$\alpha^{12}(k) = -\alpha^{21}(k) = i\eta \frac{q^2 n}{m} \frac{y}{1+y^2} \left[ \frac{(z - z_+)S(z_+) - (z - z_-)S(z_-)}{z_+ - z_-} \right], \quad (\text{A 14g})$$

$$\alpha^{13}(k) = \alpha^{31}(k) = \frac{q^2 n}{m} \frac{1}{1+y^2} \frac{k_{\perp}}{k_{\parallel}} \left[ \frac{(z - z_+)z_+R(z_+) - (z - z_-)z_-R(z_-)}{z_+ - z_-} \right], \quad (\text{A 14h})$$

$$\alpha^{23}(k) = -\alpha^{32}(k) = -i\eta \frac{q^2 n}{m} \frac{y}{1+y^2} \frac{k_{\perp}}{k_{\parallel}} \left[ \frac{z_+S(z_+) - z_-S(z_-)}{z_+ - z_-} \right]. \quad (\text{A 14i})$$

The 3-tensor form (4.1) follows on identifying the  $ij$  component of the 3-tensor  $\mathbf{K}-\mathbf{I}$  with  $-\mu_0/\omega^2$  times the  $ij$  components of the 4-tensor (A 14), and then summing over the contributions from electrons and positrons.

## References

- Abramowitz, M. and Stegun, I. A. 1965 *Handbook of Mathematical Functions*, Dover, New York.
- Allen, M. C. and Melrose, D. B. 1982 Elliptically polarized natural modes in a pulsar magnetosphere. *Proc. Astron. Soc. Aust.* **4**, 365–370.
- Arons, J. and Barnard, J. J. 1986 Wave propagation in pulsar magnetospheres: dispersion relations and normal modes of plasmas in superstrong magnetic fields. *Astrophys. J.* **302**, 120–137.
- Gedalin, M. E. 1993 Linear waves in relativistic anisotropic magnetohydrodynamics *Phys. Rev.* **E47**, 4354–4357.
- Gedalin, M. E. and Machabeli, G. Z. 1983 Oblique waves propagating in a relativistic electron–positron plasma. *Astrofizika* **19**, 153–159 [*Astrophysics* **19**, 91–95].
- Gedalin, M., Melrose, D. B. and Gruman, E. 1998 Long waves in relativistic pair plasma in a strong magnetic field. *Phys. Rev.* **E57**, 3399–3410.
- Godfrey, B. B., Newberger, B. S. and Taggart, K. A. 1975 A relativistic plasma dispersion function. *IEEE Trans. Plasma Sci.* **PS-3**, 60–67.
- Kazbegi, A. Z., Machabeli, G. Z. and Melikidze, G. I. 1991 On circular polarization in pulsar emission. *Mon. Not. R. Astron. Soc.* **253**, 377–388.
- Kennett, M. P. 2000 The effect of the cyclotron resonance on wave dispersion and absorption in an ultrarelativistic pulsar plasma. MSc Thesis, University of Sydney.
- Lominadze, D. G., Machabeli, G. Z. and Ussov, V. V. 1983 Theory of NP 0532 pulsar radiation and the nature of the activity of the Crab Nebula. *Astrophys. Space Sci.* **90**, 19–43.

- Lyutikov, M. 1998 Waves in a one-dimensional magnetized relativistic pair plasma. *Mon. Not. R. Astron. Soc.* **293**, 447–468.
- Machabeli, G. Z. and Usov, V. V. 1989 Cyclotron instability in the magnetosphere of the Crab Nebula pulsar, and the origin of its radiation. *Pis'ma Astron. Zh.* **5**, 445–449 [*Soviet Astron. Lett.* **5**, 238–241 (1990)].
- Melrose, D. B. 1997 Response of a relativistic, anisotropic, thermal plasma: II. Magnetized particles. *J. Plasma Phys.* **58**, 721–734.
- Melrose, D. B. and Stoneham, R. J. 1977 The natural modes in a pulsar magnetosphere. *Publ. Astron. Soc. Aust.* **3**, 120–122.
- Melrose, D. B., Gedalin, M. E., Kennett, M. P. and Fletcher, C. S. 1999 Dispersion in an intrinsically-relativistic, one-dimensional, strongly-magnetized pair plasma. *J. Plasma Phys.* **62**, 233–248.
- Mikhailovskii, A. B., Onischenko, O. G., Suramlshvili, G. I. and Sharapov, S. E. 1982 The emergence of electromagnetic waves from pulsar magnetospheres. *Pis'ma Astron. Zh.* **8**, 685–688 [*Soviet Astron. Lett.* **8**, 369–371].
- Polyakov, P. A. 1983 A new kind of oscillations in a relativistic plasma. *Zh. Eksp. Teor. Fiz.* **85**, 1585–1589 [*Soviet Phys. JETP* **58**, 922–924].
- Polyakov, P. A. 1997 Theory of waves in a magnetized relativistic plasma. *Plasma Phys. Rep.* **23**, 172–174.
- Shabad, A. E. 1975 Photon dispersion in a strong magnetic field. *Ann. Phys. (NY)* **90**, 166–195.
- Tsyтович, V. N. and Kaplan, S. A. 1972 Relativistic turbulence in pulsars. *Astrofizika* **8**, 441–460 [*Astrophysics* **8**, 260–272].
- Volokitin, A. S., Krasnoselskikh, V. V. and Machabeli, G. Z. 1985 Waves in a relativistic electron-positron plasma in pulsar. *Soviet J. Plasma Phys.* **11**, 531–538.